SSC20-WKI-09

A Non-Hohmann Method for Orbital Element Database Pre-Processing

William O. S. Hudnut, Cameron P. Mehlman, Kurt S. Anderson
Department of Mechanical, Aerospace, and Nuclear Engineering
Rensselaer Polytechnic Institute
JEC 2049 Jonsson Engineering Center
110 8th Street Troy, NY 12180 USA
802-356-0329
hudnuw@rpi.edu

May 2020

ABSTRACT

One major obstacle to successful orbital debris remediation is the determination of which pieces of debris are the most viable targets for capture and de-orbit. The viability of a target is determined by some combination of the debris' risk factor (a combination of its size, composition, and the orbit it occupies), the anticipated resource cost to find and capture the debris, and the underlying probability of successful intercept and capture of that target. The problem of selecting debris for capture by a multi-capture capable spacecraft is fundamentally a traveling salesman problem in which the traveler only has the resources to reach a very limited subset of the available destinations. Therefore, rapidly identifying the sets of destinations (i.e. pieces of debris) which are either too expensive to reach or insufficiently valuable to justify targeting will reduce the target destination set; this would significantly enhance the efficiency of the solution. This problem of intelligently reducing the space of possible solutions can be partially solved by performing a preliminary filtering and sorting of orbital debris database entries using known spacecraft orbital parameters and maneuvering ΔV-budget to reduce the number of possible destinations for an optimizer to those which are in fact accessible from the spacecraft's initial orbit. The chosen algorithm for analyzing and filtering the data is a two-burn node-to-node non-Hohmann transfer, which was used to estimate the ΔV-cost for transfer from the capture spacecraft's initial orbit to an orbit near the target piece of debris. Once the ΔV-cost was calculated for each transfer orbit, entries with excessive fuel costs were removed from consideration, and the fuel cost to access each remaining orbit was appended to its entry. This method was capable of reducing a 10,400-item list of debris to less than 100 accessible targets in under 3 seconds on an ordinary laptop computer. This reduction in database size brought the number of targets down to a practical size for processing by a more computationally expensive optimization algorithm suitable for selecting final targets for a multi-capture spacecraft.

INTRODUCTION

In 1958, the United States' Vanguard I satellite became the first man-made object to enter orbit around earth without reentering the atmosphere. Since then, due to the increase of man made objects in orbit as well as satellite collisions, the amount of detritus in orbit around earth has increased exponentially. The ESA estimates over 100 million pieces of debris orbit Earth at every moment, most are smaller than 10 cm [7]. Debris of this size creates huge risks for any space endeavor within Earth's orbit because they are difficult to avoid and travel at hypersonic speeds (up to 7.8 km/s). A collision at these speeds can cause severe damage to a spacecraft; even flecks of paint have been known to crater and crack windows. The most imminent threat from space debris is that with increasing numbers of debris in orbit, there is an increasing chance of debris perpetually colliding and breaking down into smaller pieces. As a result, vast regions of low-earth orbit (LEO) space could be deemed unusable due to fields of small yet highly dangerous particles. This hypothesized cascading of collisions yielding an exponential growth in the number of pieces of fragmented debris is also known as Kessler's Syndrome [20].

In the past, there has been little to no effort to actively reduce the amount of debris in orbit around Earth, and most proposals only target larger intact spacecraft. OSCaR (Obsolete Spacecraft Capture and Removal) is a 3-unit CubeSat satellite system designed to target, capture, and de-orbit smaller debris in LEO (of approximately 1 to 20 cm in size). OSCaR is being developed to pursue individual pieces of debris and then, capture its target using a weighted net. The debris and net is slowly pulled into the atmosphere, through the use of electromagnetic tethers [19], where they will burn up upon re-entry. The final piece of debris captured by OSCaR is deorbited along with the spacecraft as OSCaR uses its remaining fuel reserve to place itself into an eliptical orbit which dips into the atmosphere and decays.

OSCaR's target set is received from a grounded station where thousands of known pieces of debris are taken into consideration, evaluated and the final debris target set is selected. Because of the size of CubeSat satellites, OSCaR has both substantial limits on fuel and nets (each OSCaR is equipped with only 3 to 4 nets depending on the CubeSat configuration). The ephemeris data of cataloged pieces of debris in orbit around the earth is recorded by organizations such as NORAD, and can be obtained in the form of two-line elements [10]. To facilitate the greatest probability of success of the mission, this list must be reduced to those pieces of debris that require acceptable quantities of propellant to find, capture, and deorbit given an OSCaR's initial orbit. The first step in narrowing this list to the final target set is to use an algorithm that can remove pieces of debris that cannot be obtained without exceeding a given ΔV budget.

The purpose of this algorithm is to conduct a preliminary search, such that the reduced list is of a manageable size for a more accurate and computationally expensive optimizer that will determine the final targets. The sorter estimates the amount of fuel required to complete a two-burn node-to-node non-Hohmann transfer from the satellite's orbit to the debris' orbit. Debris that required more ΔV than the predetermined limit are removed from the list. The algorithm described herein does not currently consider additional propellant required for any phasing burns required to realize the subsequent OSCaR-debris rendezvous once OSCaR has placed itself in the debris piece orbit. The sorter returns a final sorted list of all debris within an optimal ΔV range of the satellite.

METHOD

The overall goal of the sorter program was to produce a reduced list of accessible rendezvous targets from a database file of debris targets, an initial set of orbital parameters for the spacecraft, and an onboard fuel budget for the spacecraft. In order to achieve this goal, four steps needed to be undertaken. First, a suitable target set had to be obtained from existing databases. Second, the data thus obtained needed to be manipulated in order to produce classical orbital parameters in a convenient format for large-scale processing. Third, an algorithmic method of calculating the delta-V required to reach a target orbit needed to be implemented. Finally, the data set needed to be cleared of impractical targets and provided in a convenient format for later processing.

Orbital ephemeris data can be retrieved from several sources, including the European Space Agency [7] and Space-Track.org [16]. These databases usually store the ephemeris data for observed satellites and debris in the two-line element (TLE) format. In order to achieve the first step of the process, the acquisition of orbital data for debris, the team turned to a M.S. thesis by Philip Hoddinott associated with the OSCaR project. This thesis was on the development of a method for retrieving open-source orbital data in a program usable by anyone familiar with basic orbital mechanics and MATLAB coding [10]. This program scanned the Space-Track.org TLE database for orbiting bodies categorized as "debris" appearing after a given date, and then generated a MATLAB data file and populated it with the TLE data thus retrieved.

Wrapper

The second and fourth steps of the process are handled in the wrapper script, which intakes the TLE data file, processes it into a useful format, passes it to the calculation algorithm, and then cleans the resultant data of target orbits which the spacecraft cannot reach. It also contains the user-input orbital parameters and ΔV budget of the OSCaR spacecraft. The processing of the incoming data is relatively simple, as the TLE format contains all the necessary information to determine the orbits of the body it concerns. The necessary processing is simply the extraction of the classical orbit elements from the appropriate indices of the TLE-formatted data set to pass to the ΔV calculation. Once transfer ΔV has been calculated for each orbit, the orbits with excessive transfer costs are deleted from the final output file.

ΔV *Calculation Algorithm*

The main objective of the filter-sorter algorithm was to provide a timely, accurate estimation of the ΔV cost to access any given piece of debris from a given initial spacecraft orbit. In order to make this estimate, some trajectory method must be chosen which suits the most likely maneuvers which will be needed to access the debris. While a Hohmann or Hohmann-like transfer orbit is usually optimal for co-planar initial and final orbits, in the case of orbital debris rendezvous it is likely that the debris will be out-of-plane with respect to the initial orbit of the spacecraft, and will have randomly oriented apse lines.

In most cases for a non-Hohmann orbital transfer, time-optimal transfers are preferred. These transfer maneuvers are usually calculated by a method which iteratively solves Lambert's problem [18]. However, while these solutions are good for exact intercepts between spacecraft, they are computationally intensive due to their iterative nature [5]. Therefore, an analytical method of trajectory and ΔV calculation was derived in order to save computational time for the purposes of the initial filtering algorithm.

The following derivation is a method to calculate the ΔV required for a two-burn non-Hohmann transfer between two inclined elliptical orbits, called orbits 1 and 2, where these orbits have arbitrarily oriented apse lines. The departure burn occurs at a point on the line of nodes on the initial orbit, and the insertion burn occurs at a point on the line of nodes on the other orbit, nominally the final orbit, opposing the initial point.

Beginning with the orbit elements for orbits 1 $(a_1, e_1, \Omega_1, \boldsymbol{i}_1, \omega_1, \theta_1)$ and 2 $(a_2, e_2, \Omega_2, \boldsymbol{i}_2, \omega_2, \theta_2)$; where a_j is the orbital semimajor axis of the trajectory, e_j is the orbital eccentricity, Ω_j is the right of ascension of the ascending node, $\boldsymbol{i}_j$ is the orbital inclination with respect to the equatorial plane, ω_j is the argument of periapsis, and θ_j is the actual anomaly; the orbital elements of the transfer orbit T $(a_t, e_t, \Omega_t, \boldsymbol{i}_t, \omega_t, \theta_t)$ must be calculated in order to determine the ΔV cost to intercept a given piece of debris.

From the orbital elements of orbits 1 and 2, the direction cosine matrices $\left[{}^{N}\mathbf{C}^{PF_1}\right]$ and $\left[{}^{N}\mathbf{C}^{PF_2}\right]$ which relate the orientations of the perifocal reference frames of orbits 1 and 2 respectively to the inertial reference frame N, with its basis vectors $\hat{n_1}, \hat{n_2}, \hat{n_3}$ can be calculated.

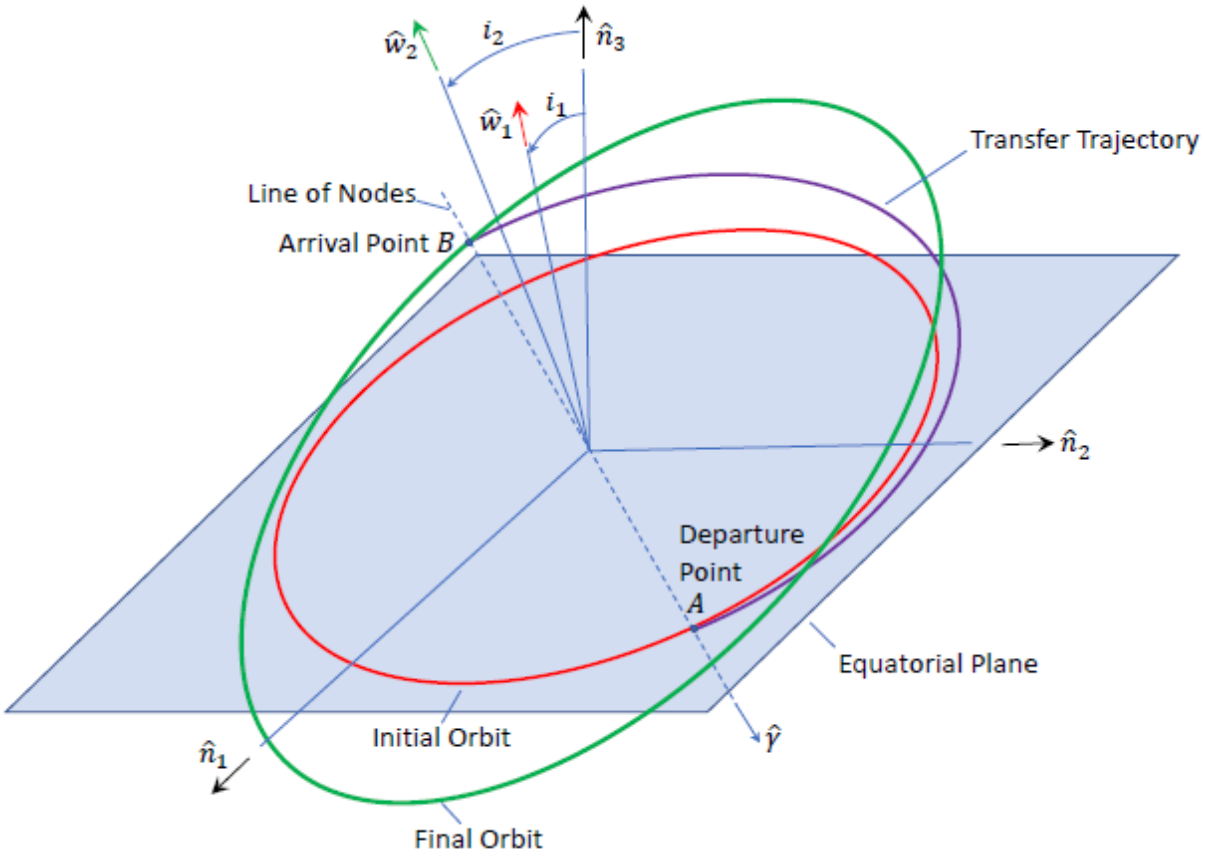

Figure 1: Inclined orbit, showing relevant unit vectors and angles

The unit vector of the line of nodes $\hat{\gamma}$ is given by

$$\hat{\gamma} = \frac{\hat{w}_1 \times \hat{w}_2}{\|\hat{w}_1 \times \hat{w}_2\|}, \tag{1}$$

as shown in figure 1 where $\hat{w}_1$, $\hat{w}_2$ are the unit vectors fixed in the inertial reference frame parallel to the orbital angular momentum vectors of orbits 1 and 2 respectively. The matrix representations of these vectors in the N reference frame correspond to the third columns of $\left[{}^{N}\mathbf{C}^{PF_1}\right]$ and $\left[{}^{N}\mathbf{C}^{PF_2}\right]$ respectively.

Defining $\theta_{\gamma 1}$ and $\theta_{\gamma 2}$ as the angles between the $\hat{p}_1$, $\hat{p}_2$ unit vectors (the vector representations of which in the N basis form first columns of $\left[{}^{N}\mathbf{C}^{PF_1}\right]$ and $\left[{}^{N}\mathbf{C}^{PF_2}\right]$ respectively) and $\hat{\gamma}$, it can be shown that the two terminal radii are $r_1(\theta_{\gamma 1})$ and $r_2(\theta_{\gamma 2})$, using the formula

$$r_j(\theta) = \frac{a_j(1-e_j^2)}{1+e_j\cos\theta_{\gamma j}}, \tag{2}$$

using appropriate values of a, e, θ.

Since orbital velocities, and therefore required ΔVs for turning maneuvers, are higher at lower orbits, the method assumes that the ΔV at the lower terminal radius is performed entirely along the flight path of the spacecraft at that point, and that all turning required for the transfer is performed at the higher terminal radius. This will adequately constrain the problem of solving for three parameters $a_t, e_t, \theta_{\gamma t}$ of the transfer orbit. It should be noted that in all situations during the implementation of this algorithm in code, the inverse tangent operation was carried out using the atan2 function to avoid ambiguities associated with the normal inverse tangent operation.

To solve for these three unknowns, the following three equations are used (assuming $r_1 < r_2$, although the equations can be modified to function using the reverse assumption):

$$K_1 = \frac{a_t(1-e_t^2)}{1+e_t\cos\theta_{\gamma t}} = \frac{a_1(1-e_1^2)}{1+e_1\cos\theta_{\gamma 1}} = r_1(\theta_{\gamma 1}), \tag{3}$$

$$K_2 = \frac{a_t(1-e_t^2)}{1-e_t\cos\theta_{\gamma t}} = \frac{a_2(1-e_2^2)}{1+e_2\cos\theta_{\gamma 2}} = r_2(\theta_{\gamma 2}), \quad (4)$$

$$\alpha_t = \tan^{-1}\frac{e_t\sin\theta_{\gamma t}}{1+e_t\cos\theta_{\gamma t}} = \tan^{-1}\frac{e_1\sin\theta_{\gamma 1}}{1+e_1\cos\theta_{\gamma 1}} = \alpha_1. \quad (5)$$

K_1 and K_2 are placeholder variables for the known values of $r_1(\theta_{\gamma 1})$ and $r_2(\theta_{\gamma 2})$, while α_t is the flight path angle of the transfer orbit at the point of departure, A, which is defined as equal to α_1, the flight path angle of the original orbit at the point of departure.

The following is a rearrangement of equation (5 which will be useful) in the solution, specifically

$$\alpha_t + \alpha_t e_t\cos\theta_{\gamma t} = e_t\sin\theta_{\gamma t}. \quad (6)$$

Equation (3) can be rearranged to acquire an expression for a_t as

$$a_t = \frac{K_1(1+e_t\cos\theta_{\gamma t})}{1-e_t^2}. \quad (7)$$

Substituting this into equation (4) yields

$$K_2(1-e_t\cos\theta_{\gamma t}) = K_1(1+e_t\cos\theta_{\gamma t}), \quad (8)$$

which can be rearranged into an expression for e_t

$$e_t = \frac{K_2-K_1}{(K_2+K_1)\cos\theta_{\gamma t}}. \quad (9)$$

Substitution of the expression for e_t into equation (6) gives

$$\alpha_t+\alpha_t\big(\frac{(K_2-K_1)\cos\theta_{\gamma t}}{(K_2+K_1)\cos\theta_{\gamma t}}\big) = \frac{(K_2-K_1)\sin\theta_{\gamma t}}{(K_2+K_1)\cos\theta_{\gamma t}} \longrightarrow$$

$$\alpha_t\big(1+\frac{K_2-K_1}{K_2+K_1}\big) = \frac{K_2-K_1}{K_2+K_1}\tan\theta_{\gamma t} \longrightarrow$$

$$\alpha_t\big(\frac{K_2+K_1}{K_2-K_1}+1\big) = \tan\theta_{\gamma t} \longrightarrow$$

$$\tan\theta_{\gamma t} = \frac{\alpha_t(2K_2)}{K_2-K_1} \longrightarrow$$

$$\theta_{\gamma t} = \tan^{-1}\big(\frac{\alpha_t(2K_2)}{K_2-K_1}\big). \quad (10)$$

Now that an expression has been found to calculate $\theta_{\gamma t}$ from known quantities K_1, K_2, α_t, the value calculated for $\theta_{\gamma t}$ can be used in equation (9), and these values for $\theta_{\gamma t}$ and e_t are used in equation (5) to get a_t.

Using the equations for orbital angular momentum, radial, and tangential velocity, specifically

$$h = a(1-e^2), \quad (11)$$

$$v_r = \frac{\mu}{h}e\sin\theta, \& \quad (12)$$

$$v_\theta = \frac{\mu}{h}(1+e\cos\theta). \quad (13)$$

v_{1rA}, $v_{1\theta A}$, the radial and tangential velocities of orbit 1 at departure point A; v_{trA}, $v_{t\theta A}$, the radial and tangential velocities of the transfer orbit at departure point A; $v_{t\theta B}$, v_{trB}, the radial and tangential velocities of the transfer orbit at arrival point B; and v_{2rA}, $v_{2\theta B}$, the radial and tangential velocities of orbit 2 at arrival point B can all be calculated.

Since $\vec{v}_1^A \cdot \vec{v}_t^A = v_{1A}v_{tA}$ is known because the initial burn is constrained to be in the direction of the original velocity vector at point A, this can be used to find

$$\frac{\vec{v}_1^A}{v_{1A}}v_{tA} = \vec{v}_t^A, \quad (14)$$

and since ${}^N\vec{r}_1^a = {}^N\vec{r}_t^A$, ${}^N\vec{v}_t^A$ can then be found using the following manipulation

$$\{r_1^A\}_N = \big[{}^N\mathbf{C}^{PF_1}\big]\{r_1^A\}_{PF_1}, \quad (15)$$

$$\{v_1^A\}_N = \big[{}^N\mathbf{C}^{PF_1}\big]\{v_1^A\}_{PF_1}, \quad (16)$$

$${}^N\vec{v}_t^A = \frac{{}^N\vec{v}_1^A}{v_{1A}}v_{tA}. \quad (17)$$

With ${}^N\vec{r}_t^A$, ${}^N\vec{v}_t^A$, $[{}^N\mathbf{C}^{PF_t}]$ can be found to be

$${}^N\vec{h}_t = {}^N\vec{r}_t^A \times {}^N\vec{v}_t^A, \quad (18)$$

$${}^N\vec{e}_t = \frac{{}^N\vec{v}_t^A \times {}^N\vec{h}_t}{\mu} - \frac{{}^N\vec{r}_t^A}{r_{tA}}. \quad (19)$$

Using these values, the perifocal frame unit vectors and the direction cosine matrix of the transfer orbit can be quickly assembled:

$$\hat{p}_t = \frac{{}^N\vec{e}_t}{e_t}, \quad \hat{w}_t = \frac{{}^N\vec{h}_t}{h_t}, \quad \hat{q}_t = \hat{w}_t \times \hat{p}_t,$$

$$\big[{}^N\mathbf{C}^{PF_t}\big] = \big[\hat{p}_t, \hat{q}_t, \hat{w}_t\big],$$

which can be used to get

$$\{v_t^B\}_N = \left[{}^N\mathbf{C}^{PF_t}\right]\{v_t^B\}_{PF_t}. \tag{20}$$

The following relation is also found

$$\{v_2^B\}_N = \left[{}^N\mathbf{C}^{PF_2}\right]\{v_2^B\}_{PF_2}. \tag{21}$$

$\Delta V_1 = \left\| {}^N\vec{v}_t^A - {}^N\vec{v}_1^A \right\|$, and $\Delta V_2 = \left\| {}^N\vec{v}_2^B - {}^N\vec{v}_t^B \right\|$. The sum of these two values, ΔV_1 and ΔV_2, is the total cost of the transfer maneuver, ΔV_{tot}.

The above method was implemented as a function in MATLAB R2018b, and used to estimate the individual ΔV to transfer from a specified initial orbit to each orbit in a target data set.

RESULTS

When the algorithm was given a low-eccentricity initial orbit that intersected an area of space densely populated with debris, often 20 or more suitable pieces of debris were found (pieces that could be reached within the propellant budget). When an initial orbit with the orbital elements $a = 7.287 * 10^6$m$, e = 0.00014, \Omega = 90°, \omega = 230°, i = 98°$ and maximum ΔV of 450m/s was put into the algorithm a total of 23 possible pieces of debris were returned. The initial list of two-line elements used by the code is a list of all of NORAD's non-protected cataloged objects in orbit around earth between 1960 to 2020. The distribution of how many of these pieces and what range of ΔV is required to maneuver to the debris orbit can be seen in figure 2.

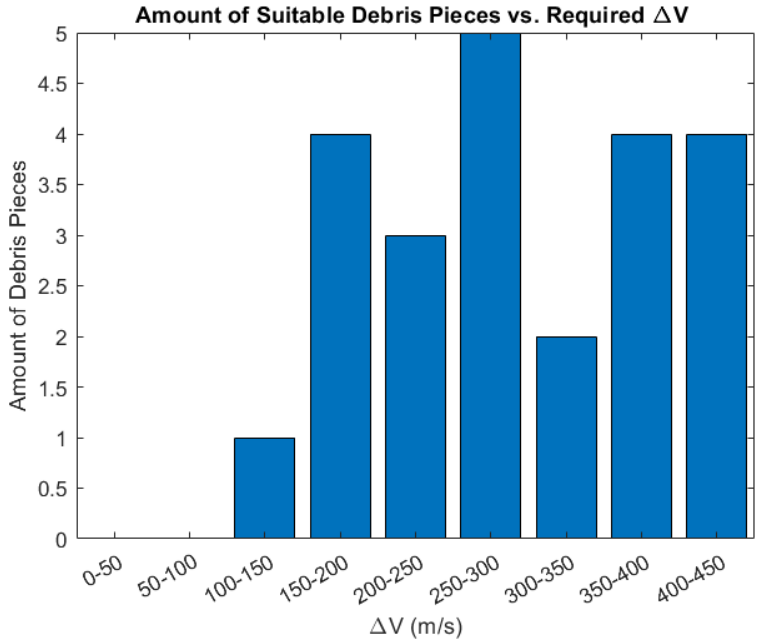

Figure 2: Suitable Pieces of Debris vs. ΔV range

The orbital elements of the final list of debris have a minimal differential from the initial orbital elements except for argument of periapsis. However, because the orbits will nominally be nearly circular, changing the argument of periapsis should require a minor amount of ΔV, even if the change in angle is greater than one radian. Because the maximum ΔV is small in relation to the ΔV required for large orbital maneuvers, the similarity between the final list of elements and the initial orbit is expected.

In order to evaluate the results of the sorting algorithm, some expectations are required for where to expect the highest amount of suitable debris for de-orbit. Using data from the ESA's MASTER software, the distribution of debris in Earth's orbit can be analyzed. A diagram plotting the spatial debris density within Earth's orbit against altitude and angle of declination can be seen below.

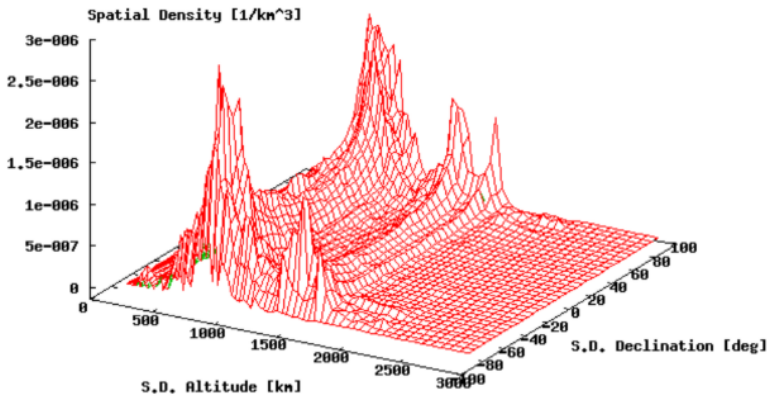

Figure 3: Spatial Debris Density vs. Altitude and Declination [2]

This data from Figure 3 shows that the densest areas of debris are between 800 and 1000 kilometers of altitude, and peaks at an angle of declination of approximately $98°$.

When the filter-sorter algorithm was run with an initial orbit with near 0 eccentricity, an inclination of $98.6°$, semi-major axis of 7.287×10^6 meters, maximum ΔV of 450 m/s and varying right ascension of ascending node between $0°$ and $180°$ with step size of $1°$ the following results were obtained. The angle of periapsis is not relevant because the orbit is near circular. The same initial list of all cataloged items between 1960 and 2020 was also used.

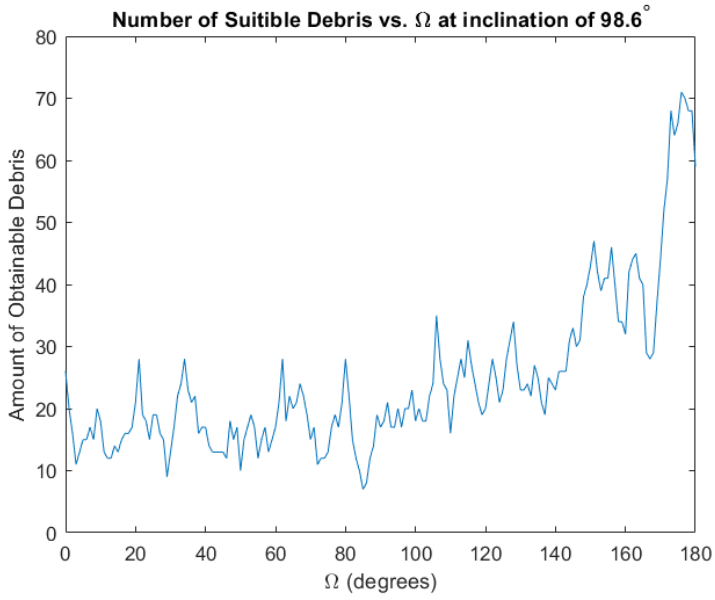

Figure 4: Number of suitable pieces of debris vs. right ascension of ascending node ($i = 98.6°$)

The data in Figure 4 shows an average of approximately 20 pieces of debris at most values of Ω, with a sharp increase as Ω approaches $180°$. The considerable amount of obtainable debris at all values of right ascension of ascending node coincides with the ESA data from Figure 3.

When a similar simulation was run using an inclination of $0°$, a very different result was obtained. In Figure 5 it is seen that the average amount of debris within a suitable range of the initial orbit is about 1 to 2 pieces of debris, and multiple orbits have no debris within range of the initial orbit. Again, this this strongly correlates with the data obtained from the ESA and indicates that the sorter algorithm is accurately identifying possible targets given OSCaR's initial orbit.

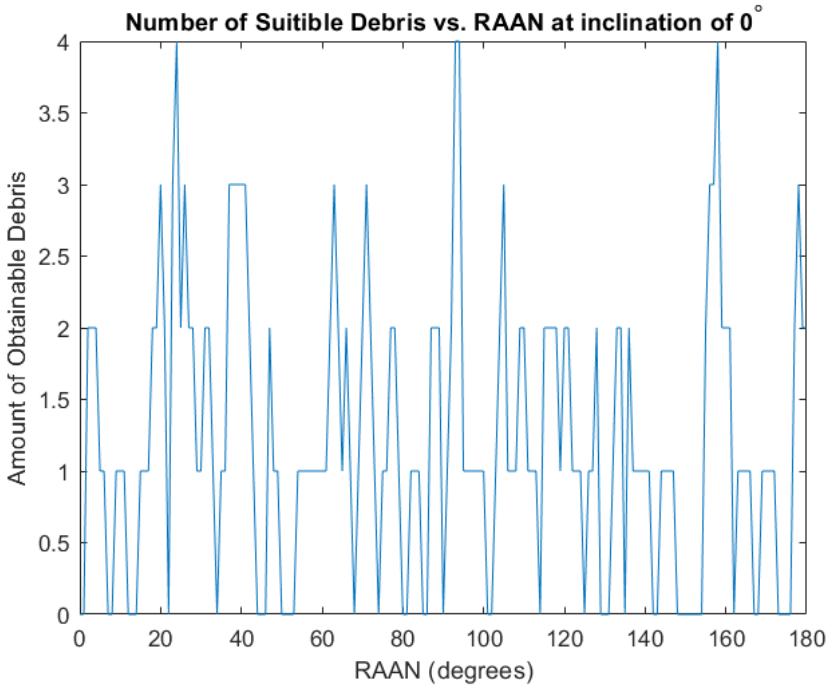

Figure 5: Number of suitable pieces of debris vs. right ascension of ascending node ($i = 0°$)

In addition to accurately identifying possible targets, the algorithm is quite fast. In testing on a laptop computer running Windows 10 on an Intel i7-6700HQ at 2.60 GHz with 16 GB of RAM, the wrapper program was able to parse and sort a 10,400 item database down to the same list of 82 accessible orbits from an initial near-circular orbit at 800 km altitude, $180°$ right ascension, and $98.6°$ inclination, with 450 m/s ΔV, in an average of 2.0966 seconds over 10 trials.

CONCLUSIONS

The goal of this sorter program was to reduce orbital debris ephemeris data files down to a size suitable for use by a more complex and accurate analysis method designed to select the targets and generate maneuvers for a multi-capture spacecraft, based on the spacecraft's initial orbit. This objective has clearly been achieved: with the 450 m/s fuel budget allocated for the OSCaR multi-capture CubeSat [2], fewer than 100 debris items were found for any initial orbit out of the 10,400 debris TLE files downloaded from Space-Track.org [16]. While this is still a large number of nodes, it is a greater than hundredfold reduction in problem size and a huge boon to any attempt to produce a viable target set for a multi-capture, or even single-capture, spacecraft.

A valuable feature of the wrapper program is that it was made to be adaptable to database

files in any format. It was designed to use the files output by Paul Hoddinott's thesis code [10], but so long as MATLAB can parse the file type, it can accept files formatted in any manner, simply by altering the file indices which are passed to the ΔV algorithm by the wrapper. So long as the code's user is familiar with the inputs required by the ΔV algorithm and the format of their input files, any input format can be used, making this program applicable for any project which would need its capabilities.

It is worth noting, however, that the algorithm is not without flaws. Specifically, the ΔV algorithm only used the two-burn node-to-node non-Hohmann transfer algorithm for its transfer ΔV estimation. While this is a good transfer solution for two elliptical orbits with significant differences in inclination, there are some cases where it is not optimal. One of these is a near-coplanar case. If the spacecraft is in an orbit with very small variance in inclination, but large variance in altitude, from the orbit of a piece of debris, a Hohmann-like periapsis or apoapsis transfer will likely have a lower ΔV cost than the node-to-node transfer. The other major case is if either the initial or target orbit is in a highly eccentric orbit. This case will, however, generally not be a concern, as even an optimal transfer between such orbits will invariably require more propellant than a small capture satellite such as OSCaR will carry, and as such they are unlikely to be valid targets for such an operation.

However, given that most of the debris with which the OSCaR spacecraft is concerned with are in low-eccentricity orbits within a well-constrained band of altitudes, and that the improvement of efficiency of a Hohmann-like transfer in the case of a coplanar orbit is small due to the low eccentricities of the expected target orbits, this issue is unlikely to cause significant losses in ability to identify targetable debris, and was accepted in order to reduce computational time. Solving for a Hohmann-like transfer would require multiple additional solutions, to check for transfers from the periapsis and apoapsis of the initial orbit, and to the periapsis and apoapsis of the target orbit, as well as any other points that might actually be optimal. While optimal solutions for transfers between close elliptic orbits have been promulgated, such as the method put forward by Jean-Pierre Marec in his doctoral thesis [12], they are iterative methods which would significantly increase the computational cost of this algorithm.

References

[1] Australian Space Academy. (n.d.). Retrieved from http://www.spaceacademy.net.au/watch/track/orbspec.htm

[2] Baker, J., Canter T., Gollin B., Kirchner C., Lyons J., Roman J., Shen J., (2016). OSCAR II Critical Design Report. Rensselaer Polytechnic Institute

[3] Battin, R. H. (1999). *An Introduction to the Mathematics and Methods of Astrodynamics* (2nd ed.). Reston, VA: American Institute of Aeronautics and Astronautics.

[4] Chobotov, V. A., Karrenberg, H. K., Chao, C., Miyamoto, J. Y., & Lang, T. J. (1991). *Orbital Mechanics* (V. A. Chobotov, Ed.). Washington, DC: American Inst. of Aeronautics and Astronautics.

[5] Der, G. J. (2011). *The Superior Lambert Algorithm.* Retrieved from AMOS Technical Conference website: https://www.amostech.com/TechnicalPapers/2011/Poster/DER.pdf, on 5 June 2019

[6] Edfors, A. (2010). COE Visualizer Tool (Version 1.01) [Computer software]. Retrieved June 19, 2019.

[7] ESA Meteoroid and Space Debris Terrestrial Environment Reference (2020)

[8] *Space Debris by the Numbers* Retrieved from ESA website: https://www.esa.int/Safety_Security/Space_Debris/Space_debris_by_the_numbers, on 12 May 2020

[9] Gooding, R. H. (1990). *A Procedure for the Solution of Lambert's Orbital Boundary Value Problem.* Celestial Mechanics and Dynamical Astronomy, 48, 145-165. Retrieved June 6, 2019.

[10] Hoddinott, P. (2018). *Tracking of Space Debris from Publically Available Data.* Thesis.

Rensselaer Polytechnic Institute, Troy, NY.

[11] Leitmann, G., et al. (1962). *Optimization Techniques With Applications to Aerospace Systems* (G. Leitmann, Ed.). London: Academic Press.

[12] Marec, J. P. (1967). *Transferts Optimaux Entre Orbits Elliptiques Proches* (Doctoral thesis, Faculty of Sciences of Paris, 1967) (NASA, Trans.). Chatillon: Office National D'Études et de Recherches Aérospatiale

[13] Oldenhuis, Rody, orcid.org/0000-0002-3162-3660. "Lambert" v1.3.0.0, 2019-06-05. MATLAB Robust solver for Lambert's orbital-boundary value problem. https://nl.mathworks.com/matlabcentral/fileexchange/26348

[14] Peet, M. M. (n.d.). *MAE 462 Lecture 8: Impulsive Orbital Maneuvers.* Lecture. Retrieved May 31, 2019, from http://control.asu.edu/Classes/MAE462/462Lecture08.pdf

[15] Peet, M. M. (n.d.). *MAE 462 Lecture 9: Bi-elliptics and Out-of-Plane Maneuvers.* Lecture. Retrieved May 31, 2019, from http://control.asu.edu/Classes/MAE462/462Lecture09.pdf

[16] SAIC (n.d.). Two-Line Element Bulk Database. Retrieved Summer 2019, from http://www.space-track.org.

[17] Stahl, M., & Raghavan, M. (n.d.). SCATTERBAR3 (Version 1.0.0.1) [Computer software]. Retrieved June 19, 2019, from https://www.mathworks.com/matlabcentral/fileexchange/1420-scatterbar3

[18] Sun, F., & Vinh, N. X. (1983). Lambertian Invariance and Application to the Problem of Optimal Fixed-Time Impulsive Orbital Transfer. Acta Astronautica, 10(5-6), 319-330. doi: 10.1016/0094-5765(83)90083-8

[19] Tethers Unlimited. http://tethers.com

[20] Corbett, J. Micrometeoroids and Orbital Debris (MMOD). August 6, 2017, from https://www.nasa.gov/centers/wstf/site_tour/remote_hypervelocity_test_laboratory/micrometeoroid_and_orbital_debris.html